Model of neutron-production rates from femtosecond-laser–cluster interactions

P. B. Parks, T. E. Cowan, R. B. Stephens, and E. M. Campbell
General Atomics, P.O. Box 85608, San Diego, California 92186-5608
(Received 10 January 2001; published 16 May 2001)

Solid deuterium clusters provide a new type of target for laser-matter interactions. We present a theory for the generation of laser driven Coulomb explosions that create a hot fusion-producing ion tail. We derive an initial distribution function for the exploded ions, for an arbitrary cluster-size distribution, and solve for the D-D neutron-production rate during the free expansion of these ions into a vacuum. We find good agreement between the theory and the experiment: the theory suggests an explanation for the observed saturation and drop in neutron yield beyond a definite cluster size, consistent with recent experiments by Ditmire [T. Ditmire *et al.*, Nature **398**, 489 (1999)] and Zweiback [J. Zweiback *et al.*, Phys. Rev. Lett. **84**, 2634 (2000); J. Zweiback *et al.*, Phys. Rev. Lett. **85**, 3640 (2000)].

DOI: 10.1103/PhysRevA.63.063203 PACS number(s): 36.40.−c, 36.40.Gk

I. INTRODUCTION

The absorption of ultrashort high-intensity laser pulses in gases at near atmospheric pressures is very ineffective. The main heating mechanism is above-threshold ionization (ATI) [1]; a collisionless process in which laser energy can be transferred directly to an electron subsequent to its ionization, provided the time to ionize the electron exceeds a few laser cycle times. At high laser powers $I \geqslant 10^{16}\,\mathrm{W/cm^2}$ the time criterion is satisfied only for $Z>1$ gases capable of multiple ionization. However, the energy distribution of ATI heated electrons is such that the average energy gained never exceeds ~60 eV in helium gas illuminated by a laser intensity of $I \sim 10^{17}\,\mathrm{W/cm^2}$. The electron energy is less for higher Z gases due to the energy drain associated with the production of higher ionization states.

Laser absorption is greatly enhanced in gases containing solid atomic clusters [1]. A cluster is an aggregate of atoms ($\sim 10^3 - 10^4$ atoms/cluster) bound together by their mutually attractive van der Waals forces. Clusters are frequently formed by nucleation when a cold, high-pressure gas jet undergoes further expansion cooling in a supersonic nozzle. When a cluster plume is illuminated by laser light field ionization sets free initial electrons, forming a high-density plasma ball. Due to the high electron-ion scattering rate, collisional, or inverse bremsstrahlung heating dominates light absorption, which is much greater than the ATI absorption process.

Extensive experimentation with large (~10 nm diameter) rare-gas clusters have been reported by Ditmire *et al.* and later by Zweiback *et al.* using a laser having a 130-fs pulsewidth centered at 825 nm, and a peak intensity of $\sim 10^{16}\,\mathrm{W/cm^2}$ [1]. The laser-cluster interaction produced a dense ball of plasma with high initial electron temperatures in the 100 to 1000 eV range, far above that of the neutral gas with equivalent volume-averaged mass density. The expanding plasma ball creates an ambipolar potential, which in turn accelerates the ions to high energies $\sim ZT_e$ where Z is the mean ion charge state. A zero-dimensional cluster disassembly model [1] supports these results, and elucidates many general features of the ionization and heating of moderately high-Z clusters. The dynamics of the cluster plasma ball appear to be governed by a balance between collisional heating and expansion cooling. An interesting ''resonance-absorption'' peak occurs momentarily during the expansion when the plasma electron density passes through a resonance point $\omega_{pe}^2 = 3\omega^2$ where $\omega_{pe} = (e^2 n_e/\varepsilon_0 m_e)^{1/2}$ is the electron plasma frequency, and ω is the laser frequency. Because the wavelength of the light is much larger than the diameter of the cluster the electric field $\mathcal{E}_L$ can be taken as uniform. Accordingly, the cluster plasma acts like a spherical dielectric with an internal electric field given by [1]

$$\mathcal{E}_{\mathrm{in}} = \frac{3}{2+\varepsilon(\omega)}\,\mathcal{E}_L\,, \tag{1}$$

where the plasma dielectric constant is given by $\varepsilon(\omega) = 1 - \omega_{pe}^2/\omega^2$. Strong collisional absorption results at the resonance point $\omega_{pe}^2 = 3\omega^2$ when the singularity is resolved by electron-ion collisions.

The use of a frequency-dependent linear dielectric constant has a limited application, however. It is meaningful only when the time scale over which the cluster electron density changes is longer than a few laser cycle times. Although this condition is marginally satisfied in the case of moderately high-Z clusters, a different regime presents itself when high-intensity laser pulses irradiate *hydrogen clusters*. As shown in Sec. II, the electron dynamics under the action of the laser field can proceed on a time scale much faster than the wave frequency, and cluster disassembly is altogether quite different.

Our focus in this paper is on laser interaction with a hydrogenic cluster medium. We are motivated to explain the first experimental results on fusion neutron production reported by Ditmire *et al.* [2] and Zweiback *et al.* [3] when an intense 35-fs laser pulse irradiated a deuterium cluster jet. Measurements of the 2.45-MeV neutron burst from the $\mathrm{D+D \rightarrow He^3} + n$ reaction seem to suggest that the ions were created by Coulomb explosion events. Simply put, under the action of intense-laser light the electrons are driven out of the cluster, uncovering bare-ion charge. The ions subsequently explode under their own space-charge forces. Ions ejected from different clusters collide with each other to cause fusion reactions. The laser-cluster interaction is a novel ''beam-

beam'' fusion approach to neutron generation, and is of contemporary interest as a potential subnanosecond neutron source for time, resolved material damage studies [3,4].

This paper presents an *ab initio* calculation of the neutron yield expected from the interaction of an intense-laser pulse with hydrogenic cluster medium. The first part of this paper describes a naive model for the behavior of the cluster electrons under the action of the laser light, Sec. II. Because the electron dynamics in the laser field is nonlinear, collective phenomena can only be studied more thoroughly with the help of detailed three-dimensional (3D) numerical simulations. In Sec. III we present a model for the ion-Coulomb explosion phase. Because of their high density, atomic clusters can be very efficient at absorbing laser energy and generating fast ions by the Coulomb explosion process. Disregarding collisional heating, the remainder of the absorbed laser energy needed to create a bare-ion cluster is partially converted to the ions with an ideal efficiency shown below in Eq. (14),

$$\frac{(\text{ion kinetic energy})}{(\text{absorbed laser energy})}=\frac{32}{47}=68\%. \tag{2}$$

The actual partition efficiency may be higher or lower depending on electron collective interaction with the laser light subsequent to their ejection from the cluster. In Sec. IV we will obtain the distribution function for the ions during their free expansion into the vacuum. From this distribution we will evaluate the fusion-reaction rate and the neutron yield. The model predicts a neutron yield as a function of cluster size that is in reasonable agreement with the Ditmire-Zweiback (DZ) experiments, without accounting for attenuation of the laser pulse as it propagates through the cluster medium (Sec. V). A conclusion, with implications for using the laser-driven Coulomb explosion of clusters as a viable neutron source, follows in Sec. VI.

II. LASER INTERACTION WITH CLUSTER ELECTRONS: A NAIVE MODEL

In order to achieve high-laser intensities and high-neutron yields the laser has to be focused to a tight cylindrical beam. In the DZ experiments the laser beam intersects a cylindrical cluster jet at right angles to it. When the laser pulse propagates into the jet it first creates a filament of ionized clusters with a length $2L_0$ and a diameter $\ll 2L_0$. Optical interferometry of the plasma filament was used to determine these dimensions, however, the filament diameter is not necessarily equal to the laser spot size d at high intensity, since ionization can take place out on the far wings of the laser beam. Therefore, the peak laser intensity and the spot size inside the cluster medium are not directly measurable. To make estimates of these important parameters we must account for ionization defocusing of the laser beam to a spot size larger than the spot size measured in the vacuum focus.

The parameter estimate begins with a brief discussion of direct laser ionization, sometimes known as field emission or tunnel ionization, depending on the laser intensity [5]. The ionization probability depends on the ''adiabaticity'' ratio $\gamma=\omega/\omega_t$ where ω is the light frequency, $\omega_t=e\mathcal{E}_L/(2m_e\phi_H)^{1/2}$ is the inverse tunneling time, $\phi_H=13.6\,\text{eV}$ is the ionization potential of the hydrogen atom, and $\mathcal{E}_L$ is the laser electric field. For plane-polarized light with $\mathcal{E}_L=\mathcal{E}_L\cos\omega t$ the amplitude can be related to laser intensity I [W cm^{-2}] by

$$\mathcal{E}_L[\text{V/m}]=2750I^{1/2}. \tag{3}$$

In the DZ experiments with laser wavelength $\lambda=820\,\text{nm}$, and nominal peak intensity along the axis of the filament $I=5\times10^{16}\,\text{W/cm}^{-2}$, one gets $\omega=2.3\times10^{15}\,\text{s}^{-1}$, $\mathcal{E}_L=6.1\times10^{11}\,\text{V/m}$, and $\gamma=0.0465$. Of interest to us in the present paper is the adiabatic limit, $\gamma\ll1$, where the probability of ionization for a hydrogen atom in the ground state can be described by Keldysh's formula [6]

$$w_i\cong1.48\tau_a^{-1}\exp\left\{-\frac{2\mathcal{E}_H}{3\mathcal{E}_L}\left(1-\frac{1}{10}\gamma^2\right)\right\}, \tag{4}$$

in which $\mathcal{E}_H=m_e^2e^5\hbar^{-4}=5.142\times10^{11}\,\text{V/m}$ is the atomic electric field at the Bohr radius $a_0=5.29\times10^{-11}\,\text{m}$. We have written the preexponential factor in Keldysh's formula in terms of the time it takes the laser field to accelerate the electron across a distance characterizing the atomic dimensions, $\tau_a=(2m_ea_0/e\mathcal{E}_L)^{1/2}$. For the above parameters of interest the wave electric field is so strong ($\mathcal{E}_L/\mathcal{E}_H\approx1.2$) that the exponential factor representing the tunneling probability is of order unity. Strictly speaking, under the action of such intense laser fields, cluster ionization is not caused by tunneling, but rather by field emission [5], i.e., classical flow over the barrier on the time scale $\sim\tau_a=0.03\,\text{fs}$. Therefore, in fast-rising laser pulses, hydrogenic cluster atoms are typically ionized in a very small fraction of a laser cycle time $\tau_L=2.73\,\text{fs}$.

However, out on the wings of the laser-intensity profile, where $\mathcal{E}_L/\mathcal{E}_H\ll1$, real tunnel ionization takes place. To obtain the ionization probability in this region we use a convenient formula that is valid in the limit where the wave field is not too strong $\mathcal{E}_L/\mathcal{E}_H\ll1$, but not too weak $\gamma\ll1$ [7]

$$w_i\cong2\omega_H\left(\frac{3}{\pi}\right)^{1/2}\left(\frac{\mathcal{E}_L}{\mathcal{E}_H}\right)^{3/2}\exp\left\{-\frac{2\mathcal{E}_H}{3\mathcal{E}_L}\left(1-\frac{1}{10}\gamma^2\right)\right\}, \tag{5}$$

Here, $\omega_H=2.07\times10^{16}\,\text{s}^{-1}$ is the hydrogen-ionization energy is frequency units. We note from Fig. 2 of Ref. [2] that the boundary of the interferometric fringe shift column seems to be located at a radius between 100 to 200 μm, which we identify as the ionization radius—to be definite the point where the ionization level is about 10% or $\int w_i dt\sim0.1$. To evaluate this integral, and thus deduce the peak laser electric field and intensity at the ionization radius, we assume that the temporal profile of the laser intensity is a Gaussian with a full width at half maximum (FWHM) pulse width $\tau_{\text{pulse}}=35\,\text{fs}$. We also assume that the radial profile of the laser intensity is a Gaussian with FWHM spot diameter d. Given the above information, and the total laser energy delivered, 100–120 mJ, we estimate that the peak laser intensity in the cluster medium lies somewhere in the range, $I_0\approx(4-8)$

$\times 10^{16}\,\mathrm{W/cm^2}$, and the spot size $d \approx 40-80\,\mu\mathrm{m}$. We will use these laser parameters together with the following nominal cluster parameters form the DZ experiments:

solid deuterium density, $n_{\mathrm{sol}} \sim 5.89\times 10^{22}\,\mathrm{cm}^{-3}$,
cluster radius, $r_c \sim 2$ nm,
number of atoms (ions) per cluster, $N_c \sim 3000$,
cluster density, $n_{\mathrm{clust}} \sim 10^{16}\,\mathrm{cm}^{-3}$,
initial ion density, $n_{i0} = N_c n_{\mathrm{clust}} \sim 3\times 10^{19}\,\mathrm{cm}^{-3}$,
average distance between clusters, $l_c \sim n_{\mathrm{clust}}{}^{-1/3} \sim 50$ nm,
smallest dimension of cluster medium $d \sim 40-80\,\mu$m.

Having established the important parameters we now turn to the physics of the laser interaction after ionization. The separation of the cluster electrons from the immobile ions is characterized by an ''instability'' when the electric field of the wave reaches certain amplitude exceeding the peak coulomb field for separation. The dynamics of the separation are described mathematically by making a simplifying assumption: the electrons move coherently under the action of *both* forces. We thus envision two interpenetrating, uniformly charged spherical clouds; the electron-charge distribution remains rigid, uniform, and spherical during its translation through the immobile ion cloud. Let the center of the ion cloud be located at the origin. The center of the electron cloud is located at the displacement distance x. Since the electron cloud has uniform density $n_e = n_{\mathrm{sol}}$ the electrostatic restoring force can be conveniently expressed as a surface integral [8]

$$\vec{F} = e n_{\mathrm{sol}} \int \Phi \hat{\mathbf{n}} dS, \tag{6}$$

where the electrostatic potential Φ is associated with the electric field $\mathcal{E} = -\nabla\Phi$ due to the ion-charge distribution only, and $\hat{\mathbf{n}}$ = the unit outward normal on the surface of the electron cloud. Let us define a normalized displacement distance $\xi = x/2r_c$. Then as long as the two charge distributions are overlapping $(-1 \leqslant \xi \leqslant 1)$ the result of the surface integration yields

$$F_x = -\frac{q^2}{16\pi\varepsilon_0 r_c^2}\,\mathrm{sgn}(\xi)(2\xi^4 - 9\xi^2 + 8|\xi|), \tag{7}$$

where $q = eN_c$ is the total ion charge residing in the cluster, and we note that F_x is like a ''restoring force'' since $F_x(\xi) = -F_x(-\xi)$. The mechanical motion of the electron-cloud displacement x is given by the force equation

$$\frac{d^2x}{dt^2} + \frac{e\mathcal{E}_{\mathrm{sur}}}{4m_e}\,\mathrm{sgn}(\xi)(2\xi^4 - 9\xi^2 + 8|\xi|) = \frac{-e\mathcal{E}_L(t)}{m_e}, \tag{8}$$

where we normalized the restoring force to the electric field at the surface of a bare-ion cluster

$$\mathcal{E}_{\mathrm{sur}} = \frac{q}{4\pi\varepsilon_0 r_c^2} = \frac{e n_{\mathrm{sol}} r_c}{3\varepsilon_0}. \tag{9}$$

Frictional drag caused by collisions with the immobile ion background does not significantly alter the dynamics, and therefore it will be disregarded. During the slow-rising part of the laser pulse that can extend over a several-cycle period, the electric field may be small enough to consider small displacements $|\xi| \ll 1$. In that case we can linearize the restoring force so that Eq. (8) goes over to the harmonic oscillator equation,

$$\frac{d^2x}{dt^2} + \bar{\omega}_{pe0}^2 x = \frac{-e\mathcal{E}_L(t)}{m_e}. \tag{10}$$

Here we define a ''reduced'' plasma frequency $\bar{\omega}_{pe0} = \omega_{pe0}/\sqrt{3}$, with $\omega_{pe0} = 1.37\times 10^{16}\,\mathrm{s}^{-1}$ being the electron-plasma frequency at the solid (deuterium) cluster density. The Fourier representation of the displacement is

$$x(\omega) = -\frac{e\mathcal{E}_L(\omega)/m_e}{\bar{\omega}_{pe0}^2 - \omega^2}. \tag{11}$$

Because the laser pulse has virtually no spectral components near the reduced plasma frequency $(\bar{\omega}_{pe0}^2/\omega^2 \approx 12)$ the inertial term is negligibly small. Cloud displacement is in phase with the oscillating electric field at any moment, and because $x(\omega)$ is so far off resonance, collisional heating is not of material interest. Thus, during the pulse rise the electron cloud oscillates back and forth in the laser field without gaining any net energy from the wave, except for some collisional heating.

At some point during the pulse rise the restoring force becomes nonlinear and Eq. (10) becomes invalid, of course. Nevertheless even when nonlinearity sets in, the electron inertia in Eq. (8) is still negligible compared to the restoring force, which still balances the laser force at any given instant. This ''quasiadiabatic'' motion continues until the laser electric field force has reached a point during its cycle when it just becomes equal to the peak in the restoring force. This peak occurs at $|\xi| = \frac{1}{2}$ and it has the magnitude $(\frac{15}{32})e\mathcal{E}_{\mathrm{sur}}$. Following the moment of threshold, $|\xi| > \frac{1}{2}$, the electron cloud breaks free and escapes the pull of the ions in a fraction of a laser cycle period. Thus complete ion charge uncovering and Coulomb explosions can only be possible if $\mathcal{E}_L > (\frac{15}{32})\mathcal{E}_{\mathrm{sur}}$. This inequality, taken together with Eqs. (3) and (9), is equivalent to saying that the cluster radius r_c must be less than a certain maximum value,

$$r_c < r_{\max}(\mathrm{nm}) \equiv 1.653\times 10^{-8} I_0^{1/2}, \tag{12}$$

which depends on the peak laser intensity $I_0\,(\mathrm{W/cm^{-2}})$, in order to have Coulomb explosions in deuterium clusters.

It is straightforward to find the electron-cloud escape time, namely, the time to go from $|\xi| = 1/2$ to $|\xi| = 1$, once the threshold laser field is reached. This is

$$t_{\mathrm{esc}} = 1.96\left(\frac{r_c m_e}{e\mathcal{E}_L}\right)^{1/2}. \tag{13}$$

Inserting $r_{\max}$ for r_c in this result gives the maximum possible escape time $t_{\mathrm{esc}}^{\max} = 4.96/\omega_{pe0}$. Even at this maximum value, the change in the wave phase during escape is still not too appreciable: $\Delta\phi = \omega t_{\mathrm{esc}}^{\max} \approx 0.83 \ll \pi$. Hence, it is guaranteed that once threshold is attained, the laser electric field

will remain higher than the Coulomb restoring force, allowing runaway electron escape in a fraction of an oscillation.

It is easy to show that the work done by the laser electric field in liberating the electron cloud is just

$$\Delta W = \frac{q^2}{8\pi\varepsilon_0 r_c}\left(\frac{61}{80}+1\right), \tag{14}$$

where the first term is the difference in the Coulomb potential energies $W_{\rm coul}(\xi=1)-W_{\rm coul}(\xi=\frac{1}{2})$, and the last term is the energy needed to remove the cloud from $\xi=1$ to ''infinity'' (several cluster radii away). The total ion energy released $U_{\rm coul}$ from a fully exploded cluster is given by Eq. (18) in Sec. III. Hence, the ideal efficiency for conversion to ion energy $U_{\rm coul}/\Delta W$ is just the numerical constant given by Eq. (2).

Once the electron cloud is liberated, it begins to quickly smear out and overlap other electron clouds from neighboring clusters. The result is that the ionized cluster filament becomes a plasma, in the usual sense that the heavy-ion clusters, before exploding, are *well screened* by the electrons. This is so because the plasma-coupling parameter $g=(e^2/\lambda_{\rm Debye})(1/kT_e)\sim 0.01$ is small, i.e., screening is statistically valid because there are many electrons in a Debye sphere. Here we have estimated the Debye length $\lambda_{\rm Debye}\sim 0.02\,\mu$m for say $\sim$100 eV electrons at the electron density equal to n_{i0}. We see also that the Debye length is much smaller than the diameter of the plasma filament $d\sim 40-80\,\mu$m, which is another condition for the plasma picture to be valid. This temperature estimate comes from calculating the rate of collisional heating during the prepulse, while the electron cloud is still bound to the cluster ions.

To conclude this section we wish to draw a connection between small displacement cloud motion, as described by Eqs. (10) and (11), and the dielectric screening model described by Eq. (1). Reference [1] adopted a screening model based upon the linear-dielectric constant of the cluster plasma ball in order to study collisional heating and multiple ionization of large, rare-gas clusters. The collective motion of the electron cloud leads to a Coulomb field that partially screens out the laser field inside the cluster. The total Coulomb field at some point *P* inside the overlapping clouds is the superposition of the electric field from the ion cloud and the electron cloud.

$$\vec{\mathcal{E}}_{\rm coul} = \frac{e n_{\rm sol}}{3\varepsilon_0}(\vec{r}_{\rm ion}-\vec{r}_{\rm electron}), \tag{15}$$

where the radial vectors indicated in Eq. (15) extend from the origin of the respective clouds to the point *P*. Since, $\vec{r}_{\rm ion}-\vec{r}_{\rm electron}=\vec{x}$, the total internal electric field inside the cluster is given by

$$\vec{\mathcal{E}}_{\rm in} = \frac{e n_{\rm sol}}{3\varepsilon_0}\vec{x}+\vec{\mathcal{E}}_L, \tag{16}$$

Substituting Eq. (11) into Eq. (16) gives

$$\vec{\mathcal{E}}_{\rm in} = \frac{\vec{\mathcal{E}}_L}{1-\dfrac{\vec{\omega}_{pe0}^2}{\omega^2}}, \tag{17}$$

which is identical to Eq. (1). The validity of the linear-dielectric model for clusters is indeed limited to small displacements and low-intensity fields, as is well known in general media.

III. ION-COULOMB EXPLOSION

In this section we examine the dynamics of the Coulomb-explosion phase. Consider a spherically shaped bare-ion cluster with a uniform ion density equal to the solid density $n_{\rm sol}$. The Coulomb potential energy is given by

$$U_{\rm coul} = \frac{\varepsilon_0}{2}\int_{\rm all\ space}\mathcal{E}_0^2 d^3\vec{r} = \frac{3q^2}{20\pi\varepsilon_0 r_c} = \frac{4\pi(e n_{\rm sol})^2 r_c^5}{15\varepsilon_0}, \tag{18}$$

where $\mathcal{E}_0$ is the initial radial electrostatic electric field. The cluster ions then feel the mutually repulsive Coulomb forces and explode. After the ions are fully exploded the potential energy is transformed into kinetic energy, with mean energy per ion given by

$$\overline{E}_{\rm ion} = \frac{n_{\rm sol} e^2 r_c^2}{5\varepsilon_0}. \tag{19}$$

A deuterium cluster with radius $r_c=2.167$ nm would have $\overline{E}_{\rm ion}=1$ keV.

During the explosion the jitter motion of the ions in the laser electric field can be neglected since the ion-oscillation amplitude $\delta_{\rm ion}=e\mathcal{E}_L/m_i\omega^2\sim 10^{-2}$ nm is much smaller than a typical cluster size. Since there is no ion pressure associated with ''random'' particle velocities, the ion motion is purely radial and can be adequately described by the cold-ion momentum equation

$$m_i\frac{Dv}{Dt} = e\mathcal{E}, \tag{20}$$

where $D/Dt=\partial v/\partial t+v\,\partial v/\partial r$. From Gauss's law the changing electric field in terms of the changing cluster-ion density n_i is

$$\mathcal{E}(r,t) = \frac{e}{\varepsilon_0 r^2}\int_0^r n_i(r',t) r'^2 dr', \tag{21}$$

Divide the volume of the cluster into Lagrangian-fluid shells defined by their radius r_0, at time $t=0$, and their subsequent radius $r(r_0,t)$ at time *t*. Taking the continuity equation

$$n_i(r,t) r^2 dr = n_{\rm sol} r_0^2 dr_0, \tag{22}$$

together with Eq. (21) reduces Eq. (20) to

$$\left.\frac{\partial^2 \xi}{\partial t^2}\right|_{r_0} = \frac{\omega_{pi0}^2}{3\xi^2}, \tag{23}$$

where we have defined a normalized radius $\xi = r(r_0,t)/r_0$, with $\omega_{pi0} = (e^2 n_{\rm sol}/\varepsilon_0 m_i)^{1/2}$ being the initial ion plasma frequency. If we apply the initial conditions $\xi = 1$, $\partial\xi/\partial t = 0$ at $t = 0$, we obtain an implicit equation for $\xi(r_0,t)$

$$\sqrt{\xi^2 - \xi} + \sinh^{-1}[(\xi - 1)^{1/2}] = \sqrt{\tfrac{2}{3}}\,\omega_{pi0} t, \tag{24}$$

and the velocity of a Lagrangian shell with time becomes

$$v(r_0,t) = \sqrt{\tfrac{2}{3}}\,\omega_{pi0} r_0 \left(1 - \frac{1}{\xi(t)}\right)^{1/2}. \tag{25}$$

Note that the characteristic time scale of the explosion is the inverse ion plasma frequency: the time to double the radius of a deuterium cluster is 12.4 fs or about 4.5 laser cycle times. When the cluster is fully exploded ($\xi \to \infty$) the ion energy approaches the asymptotic limit

$$E(r_0) = \frac{e^2 r_0^2 n_{\rm sol}}{3\varepsilon_0}. \tag{26}$$

The total energy is conserved since the final kinetic energy for a fully exploded cluster,

$$U_{kin} = \int_0^{r_c} n_{\rm sol} E(r_0) 4\pi r_0^2 dr_0, \tag{27}$$

equals the initial potential energy $U_{\rm coul}$ given by Eq. (18). We also see from Eq. (26) that the ions residing on the surface of the cluster ($r_0 = r_c$) acquire the most kinetic energy, namely $E_{\rm sur} = (\frac{5}{3})\overline{E}_{\rm ion}$. In convenient units, with energy in keV and radius in nm this relation for deuterium can be written as

$$E_{\rm sur} = 0.355 r_c^2, \tag{28}$$

$$r_c = 1.678 E_{\rm sur}^{1/2}. \tag{29}$$

The distribution of ion energies from a single cluster is then $\mathcal{F}(E) = (dN/dr_0)/(dE/dr_0)$ or

$$\mathcal{F}(E) = \frac{2\pi(3\varepsilon_0)^{3/2} E^{1/2}}{e^3 n_{\rm sol}^{1/2}} \quad \text{if } E \leqslant E_{\rm sur}$$
$$= 0 \quad \text{if } E \geqslant E_{\rm sur}. \tag{30}$$

Of course the clusters have many different sizes. When trying to determine the fusion reactivity from cluster ions interacting with ions ejected from other clusters in the ensemble the cluster-size distribution is important. Suppose the clusters can be characterized by a radius-distribution function $g(r_c)$, the number of clusters per unit increment in cluster radius. We normalize g such that

$$n_{\rm clust} = \int_0^\infty g(r_c) dr_c. \tag{31}$$

After the ejected ions have traversed the intercluster distance l_c the cluster graininess is in a way ''forgotten'' and the initial ion density is locally smoothed out. The smoothing time is essentially instantaneous on the subsequent ion-expansion time scale that is longer by the ratio $d/l_c \gg 1$. The initial ion density at position $\vec{x}$ would then be

$$n_{i0}(\vec{x}) = \frac{4\pi n_{\rm sol}}{3} \int_0^\infty r_c^3 g(r_c,\vec{x}) dr_c. \tag{32}$$

Note that this density is inferred by measuring the electron density, for example, by optical interferometry. Hence it includes the ions of disassembled clusters that do not undergo a Coulomb explosion, $r_c > r_{\rm max}$. We can rewrite Eq. (32) as

$$n_{i0}(\vec{x}) = 4\pi n_{\rm sol} \int_0^\infty g(r_c,\vec{x}) dr_c \int_0^{r_c} r_0^2 dr_0. \tag{33}$$

By interchanging the order of integration, Eq. (33) can be expressed as

$$n_{i0}(\vec{x}) = 4\pi n_{\rm sol} \int_0^\infty r_0^2 dr_0 \int_{r_0}^\infty g(r_c,\vec{x}) dr_c. \tag{34}$$

Consequently,

$$\frac{dn_{i0}(\vec{x})}{dr_0} = 4\pi n_{\rm sol} r_0^2 dr_0 \int_{r_0}^\infty g(r_c,\vec{x}) dr_c. \tag{35}$$

The distribution of energies for ions ejected by Coulomb explosions ($r_c < r_{\rm max}$) is finally $f_0(E,\vec{x}) = (dn_{i0}/dr_0)/(dE/dr_0)$, or with the aid of Eq. (26) again, this becomes

$$f_0(E,\vec{x}) = \frac{2\pi(3\varepsilon_0)^{3/2} E^{1/2}}{e^3 n_{\rm sol}^{1/2}} \int_{r_{0(E)}}^{r_{\rm max}} g(r_c,\vec{x}) dr_c, \tag{36}$$

in which Eq. (26) can be inverted and then substituted for the lower limit on the integral. Although Rayleigh scattering measurements of the cluster plume can provide information on the average cluster size, the actual form of the size distribution is lacking at this time. We therefore borrow from a class of parametric forms suggested for characterizing the sizes of atmospheric aerosols and ice particles in clouds [9]. A particularly simple form used a hereafter is

$$g(r_c,\vec{x}) = \left(\frac{2}{\pi}\right)^{1/2} \frac{n_{i0}(\vec{x})}{4 r_{\rm m}^5 \pi n_{\rm sol}} r_c \exp[-r_c^2/2r_m^2], \tag{37}$$

where r_m is the radius that peaks the distribution, and the average radius is $r_{\rm avg} = (\pi/2)^{1/2} r_m$. Interestingly, this particular form yields, a Maxwellian velocity distribution, with a constant offset

$$f_0(\vec{v},\vec{x}) = n_{i0}(\vec{x}) \left(\frac{m_i}{2\pi T_*}\right)^{3/2} \{\exp[-m_i v^2/2T_*]$$
$$- \exp[-m_i v_{\rm max}^2/2T_*]\}. \tag{38}$$

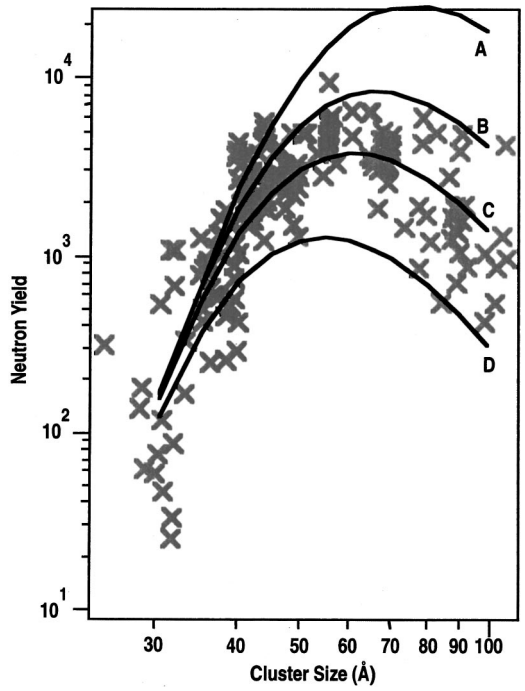

FIG. 1. Neutron yield versus average cluster diameter, $2r_{\mathrm{avg}}$. Experimental data points—circles and squares—are taken from Fig. 4 of Ref. [3]. Solid curves are calculated from Eq. (70) using similar experimental values for the plasma filament mentioned in the text, and allowing for a range of laser intensities (W/cm^2): (A) 8×10^{16}; (B) 6×10^{16}; (C) 5×10^{16}; (D) 4×10^{16}.

This distribution function contains two important parameters: the effective temperature $T_*(\mathrm{eV})$, which is related to the average cluster size

$$T_*=\frac{4en_{\mathrm{sol}}r_{\mathrm{avg}}^2}{3\pi\varepsilon_0}, \tag{39}$$

and the cutoff energy, which is related to the laser intensity $I[\mathrm{W/cm^2}]$

$$E_{\mathrm{max}}\equiv\frac{1}{2}m_iv_{\mathrm{max}}^2=9.7\,(\mathrm{keV})\left(\frac{I}{10^{17}}\right). \tag{40}$$

For example, in the DZ experiments a nominal average cluster radius $r_{\mathrm{avg}}=4$ nm gives $T_*=7.23$ keV or an average ion energy of about $(\frac{3}{2})T_*=11$ keV, which is consistent with the average ion energy determined by neutron-Doppler broadening [3]. As a check on the ion-distribution function, one can easily verify that the kinetic-energy density of the Coulomb-exploded ions is equal to the potential-energy density of the preexploded clusters, i.e.,

$$\int_0^{v_{\mathrm{max}}}(\tfrac{1}{2})m_iv^2f_0(\vec{v},\vec{x})d^3\vec{v}=\int_0^{r_{\mathrm{max}}}g(r_c,\vec{x})U_{\mathrm{coul}}(r_c)dr_c. \tag{41}$$

This distribution function seems to provide a plausible explanation for the experimentally observed neutron signal as a function of average cluster radius, illustrated in Fig. 1. Increasing the radius increases the temperature T_*, and the $D(d,n)^3$ He fusion reaction rate. This trend continues until saturation followed by a fall off in the neutron yield occurs at a certain radius. Presumably, the large-radius drop in yield is due to the reduction in the density of the fusion-producing ion tail due to the cutoff energy E_{max}. The only possible way to continue the upward trend in neutron yield with cluster size is to increase the laser intensity E_{max}, along with the cluster size. However, the enhancement of the fusion-producing ion tail eventually diminishes with laser intensity since the second term in Eq. (38) vanishes exponentially with increasing E_{max}.

The next two sections are aimed at quantifying these above hypotheses. To do so we consider in the next section how the initial distribution function derived here evolves during its free expansion. Only a small penalty in accuracy is incurred if, for the sake of mathematical simplicity, we replace our initial ion distribution given by Eq. (38) with an ordinary Maxwellian distribution function that is simply truncated for $v>v_{\mathrm{max}}$. The resulting fusion yield will then be calculated on the basis of this evolving distribution function, and it will be compared with the DZ experimental result in Sec. V.

IV. COLLISIONLESS-EXPANSION MODEL

We now consider the expansion of a fixed mass of plasma into a vacuum. In the past, most problems concerned with free expansions have treated a cloud of particles initially in the continuum, or gas-dynamic limit. Here we have a special state of affairs given our assumed cluster-size distribution: the initial distribution function of the ions is collisionless yet Maxwellian, albeit truncated. The initial ion cloud has roughly the shape of a long-thin cylinder with axial length $2L_0$ and radius $R_0=d/2\ll2L_0$. A related collisionless-expansion problem, with a different approach and objective, was considered in Ref. [10]. The collisionless approximation is reasonable here since the ion-ion collisional scattering time τ_{ii} is about two orders of magnitude longer than the characteristic radial expansion time $\tau_{\mathrm{exp}}\sim R_0/(T_*/m_i)^{1/2}\sim0.1$ ns. Similarly, the ion-electron energy exchange is also sufficiently large provided the electron temperature in the ion cloud exceeds ~100 eV at the beginning of the expansion. Hence, the ions born at each point fly away ballistically and travel in all directions. Because the laser pulse is depleted along the propagation direction, the intensity, and thus the initial ion distribution function, will vary in the axial direction. However the scale length of the variation is long compared with the radius of the filament. In addition, the pulse-propagation time along the channel path $2L_0/c\sim7$ ps is short compared to τ_{exp}. Therefore, the initial ions are created in a delta-function time pulse, and we may consider the expansion to be approximately two-dimensional (radial) at any given axial location. The evolution of the distribution function f_i can be described by the Boltzmann equation without a collision term.

$$\frac{\partial f_i}{\partial t}+\vec{v}\cdot\vec{\nabla}f_i=\delta(r)f_{i0}, \tag{42}$$

where f_{i0} is our initial ion distribution function at $t=0$. Since the axial particle motion decouples from the transverse particle motion, the distribution function for a 2D cylindrical expansion can be written in separable form

$$f_{\rm cyn}(\vec{v},\vec{r},t)=F(v_\perp,\chi,r,t)G(v_\parallel),$$
$$G(v_\parallel)=\left(\frac{m_i}{2\pi T_*}\right)^{1/2}\exp\left[-\frac{m_i v_\parallel^2}{2T_*}\right], \tag{43}$$

where r is the radial coordinate, $v_\perp$ is the transverse velocity component, $v_\parallel$ is the axial velocity component ($v^2=v_\perp^2+v_\parallel^2$), and χ is the local angle between the transverse velocity vector $\vec{v}_\perp$ and the radius vector $\vec{r}$, i.e., $v_r=v_\perp\cos\chi$, $v_\theta=v_\perp\sin\chi$. Consequently, Eq. (42) becomes

$$\frac{\partial F}{\partial t}=v_\perp\cos\chi\frac{\partial F}{\partial r}-v_\perp\frac{\sin\chi}{r}\frac{\partial F}{\partial\chi}=\delta(t)F_0, \tag{44}$$

in which

$$F_0(r,v_\perp)=n_{i0}(r)\left(\frac{m_i}{2\pi T_*}\right)\exp\left[-\frac{m_i v_\perp^2}{2T_*}\right].$$

Both $v_\perp$ and the angular momentum per unit mass, $p=rv_\theta$, are constants of motion during the expansion. For convenience, the variables $v_\perp$, χ, and r will be transformed to a new set $v_\perp$, p, and r, thus reducing Eq. (44) to the new form

$$\frac{\partial F}{\partial t}+\left(v_\perp^2+\frac{p^2}{r^2}\right)^{1/2}\left.\frac{\partial F}{\partial r}\right|_{v_\perp,p}=\delta(t)F_0. \tag{45}$$

The distribution function remains constant along a characteristic described by the equation

$$dt=\frac{dr}{\left(v_\perp^2+\frac{p^2}{r^2}\right)^{1/2}}. \tag{46}$$

By radial symmetry $F(v_\perp,\chi,r,t)=F(v_\perp,-\chi,r,t)$. Thus we only consider ion trajectories in the phase-space region $0<\chi<\pi$. In this region, ions at some position on a circle with radius r at time t are either ''inbound'' ($\cos\chi<0$) or they are ''outbound'' ($\cos\chi>0$). In-bound ions have characteristics defined by

$$t-t'=\int_r^{r'}s(s^2v_\perp^2-p^2)^{-1/2}ds, \tag{47}$$

and out-bound ions have characteristics

$$t-t'=\int_{r'}^{r}s(s^2v_\perp^2-p^2)^{-1/2}ds, \tag{48}$$

where the primed variables denote the particle's position at an earlier time in terms of its position at time t. Integrating Eq. (45) along these characteristics gives

$$F=\int_{-\infty}^{t}\delta(t')F_0[r'(t'),v_\perp]dt'. \tag{49}$$

To carry out the integration explicitly we need an initial density profile, which we take to be a Gaussian

$$n_{i0}(r)=\frac{N_i}{2\pi L_0R_0^2}\exp[-r^2/R_0^2], \tag{50}$$

with a $1/e$ core radius equal to R_0. The fixed number of exploded ions of species i in the cluster ensemble is N_i. Then for outgoing (ingoing) ions $F=F_+(F_-)$ where

$$F_\pm=\frac{N_i}{\pi L_0R_0^2}\left(\frac{m_i}{2\pi T_*}\right)\exp\left[\frac{\pm 2t(r^2v_\perp^2-p^2)^{1/2}-r^2}{R_0^2}\right]$$
$$\times\exp\left[-\frac{v_\perp^2}{v_{ti}^2}\left(1+\frac{v_{ti}^2t^2}{R_0^2}\right)\right], \tag{51}$$

and the initial ion thermal speed is $v_{ti}=(2T_*/m_i)^{1/2}$. After some rearrangement, this result can be expressed in velocity-space variables v_r,v_θ. It follows that the distribution function takes the form of a shifted bi-Maxwellian with a radial flow $u_{ir}(r,t)$:

$$f_{i,\rm cyn}=n_{i,\rm cyn}\left(\frac{m_i}{2\pi T_\perp}\right)\left(\frac{m_i}{2\pi T_\parallel}\right)^{1/2}$$
$$\times\exp\left[-\frac{m_iv_\theta^2}{2T_\perp}-\frac{m_i(v_r-u_{ir})^2}{2T_L}-\frac{m_iv_\parallel^2}{2T_\parallel}\right]=0$$
$$\text{for } v_r^2+v_\theta^2+v_\parallel^2\geqslant v_{\rm max}^2, \tag{52}$$

Expressions for the normalized radial flow velocity, transverse temperature $T_\perp(t)$, longitudinal temperature $T_\parallel$, core radius $R(t)$, and density $n(r,t)$ are given by

$$\bar{u}=\frac{u_{ir}}{v_{ti}}=\frac{r/v_{ti}t}{1+\frac{R_0^2}{v_{ti}^2t^2}},\quad T_\perp=T_*\frac{R_0^2}{R^2},\quad T_\parallel=T_*,$$

$$R=R_0\left(1+\frac{v_{ti}^2t^2}{R_0^2}\right)^{t/2},\quad n_{i,\rm cyn}=\frac{N_i}{\pi LR(t)^2}\exp\left(-\frac{r^2}{R(t)^2}\right).$$

The same type of analysis can be extended to the 3D spherically symmetric expansion, and the 1D slab expansion,

$$f_{i,\rm sph}=n_{i,\rm sph}\left(\frac{m_i}{2\pi T}\right)^{3/2}\exp\left[-\frac{m_i(v-u_{ir})^2}{2T}\right]=0$$
$$\text{for } v^2\geqslant v_{\rm max}^2,$$
$$\vec{u}=\frac{u_{ir}}{v_{ti}}=\frac{r/v_{ti}t}{1+\frac{R_0^2}{v_{ti}^2t^2}},\quad T=T_*\frac{R_0^2}{R^2},\quad R=R_0\left(1+\frac{v_{ti}^2t^2}{R_0^2}\right)^{1/2}, \tag{53}$$

$$n_{i,\mathrm{sph}}=\frac{N_i}{\pi^{3/2}R(t)^3}\exp\left(-\frac{r^2}{R(t)^2}\right).$$

$$f_{i,\mathrm{slab}}=n_{i,\mathrm{slab}}\left(\frac{m_i}{2\pi T_\perp}\right)\left(\frac{m_i}{2\pi T_\parallel}\right)^{1/2}\times\exp\left[-\frac{m_i(v_r^2+v_\theta^2)}{2T_\perp}-\frac{m_i(v_\parallel-u_{ir})^2}{2T_\parallel}\right]=0$$

$$\text{for } v_r^2+v_\theta^2+v_\parallel^2\geqslant v_{\max}^2.$$

$$\overline{u}=\frac{u_{iz}}{v_{ti}}=\frac{z/v_{ti}t}{1+\dfrac{R_0^2}{v_{ti}^2t^2}},\quad T_\parallel=T_*\frac{L_0^2}{L^2},\quad T_\perp=T_*. \tag{54}$$

$$L=L_0\left(1+\frac{v_{ti}^2t^2}{L_0^2}\right)^{1/2},\quad n_{i,\mathrm{slab}}=\frac{N_i}{\pi^{3/2}L(t)R_0^2}\exp\left(-\frac{z^2}{L(t)^2}\right).$$

Here, we define L_0 to be the initial $1/e$ half-width in the longitudinal z direction, and R_0 the fixed radius such that $L_0\ll R_0$.

Note that in all three cases the time history of the temperature in the expansion direction is the same. This can be understood from the fluid point of view. If the cloud were a collisional fluid, each fluid element with volume element V would obey the adiabatic law $TV^{(\gamma-1)}$, where γ is the adiabatic constant. In the case of the (3D) spherically symmetric expansion all three degrees of freedom participate in the expansion, therefore $\gamma=5/3$. For the cylinder expansion, only two degrees of freedom are attributable to the motion in the transverse direction, so $\gamma=2$, and for the planar expansion $\gamma=3$. Hence, in all three cases the temperature decreases with the square of the cloud dimension in the expansion direction. From the standpoint of maintaining a high-fusion reactivity during the expansion, the 3D expansion seems to be the least desirable (and hardest to realize in practice) because the temperature drop is isotropic and the density decay is the fastest. The 1D expansion is the most favorable because the temperature corresponding to the two perpendicular degrees of freedom $T_\perp$ remains constant, and also the density decay is the slowest. Such a 1D expansion could be envisioned by creating a sheetlike-cluster beam right from the beginning by using a tapered supersonic nozzle section with a slit-shaped exit, instead of a round hole. One could then use a cylindrical lens to focus the laser to a cylindrical beam normal to the plane of the cluster sheet. This would form a shell-like plasma cloud that subsequently undergoes a nearly 1D expansion.

There may be a concern that the ion temperature anisotropy would drive a well-known transverse electromagnetic instability, which would tend to drive the distribution function toward isotropy, $T_\perp\approx T_\parallel$. In the case of the cylindrical expansion the instability generates an electric field in the axial direction, a magnetic field in the azimuthal direction, and the significant wavenumber k is in the radial direction. From the generalized linear dispersion relation [11], we find for our parameters of interest a purely growing mode that has a maximum growth rate

$$\gamma_{\mathrm{inst}}=\left(\frac{8}{27\pi}\frac{T_e}{T_i}\frac{m_e}{m_i}\right)^{1/2}\omega_{pi}\left(\frac{T_\perp}{m_ic^2}\right)^{1/2}\left(\frac{T_\parallel}{T_\perp}-1\right)^{3/2},$$

at

$$k=\frac{\omega_{pi}}{3^{1/2}c}\left(\frac{T_\parallel}{T_\perp}-1\right)^{1/2},$$

where ω_{pi} is the ion-plasma frequency. Evidently, the instability is probable since there are unstable wave numbers $k\geqslant R_0^{-1}$ fitting in the cylindrical plasma of radius R_0. However, for typical parameters the maximum growth rate is slow on the expansion time scale, $\tau_{\exp}\gamma_{\mathrm{inst}}\sim 10^{-3}$. Clearly, this electromagnetic instability is too benign to isotropize the ion-distribution function during expansion.

V. FUSION NEUTRON YIELD AND COMPARISON WITH EXPERIMENT

The reactivity for binary nuclear reactions has the symbolic definition,

$$\langle\sigma v\rangle=\int_{\vec{v}_1}\int_{\vec{v}_2}f_1(\vec{v}_1)f_2(\vec{v}_2)|\vec{v}_1-\vec{v}_2|\sigma(|\vec{v}_1-\vec{v}_2|)d^3\vec{v}_1d^3\vec{v}_2, \tag{55}$$

where the distribution functions of the interacting ion species are normalized to unity, and σ is the reaction cross section, which depends only on the relative speed of impact $|\vec{v}_1-\vec{v}_2|$. The fusion reaction rate per unit time and unit volume is then

$$\mathcal{R}=\frac{n_in_2}{\delta}\langle\sigma v\rangle, \tag{55a}$$

where δ is 1 for unlike species and 2 for like species. The total neutron yield from the expanding ion cloud is then

$$N_{\mathrm{neutron}}=\int_0^\infty dt\int_{\mathrm{vol}}\mathcal{R}d^3\vec{r}. \tag{56}$$

Various mathematical methods have been employed to reduce the sixfold reactivity integral to a manageable form. For example, Ref. [12] describes a general method that is particularly useful when an isotropic distribution interacts with an arbitrary anisotropic distribution. An example of that is a Maxwellian species interacting with a bi-Maxwellian, where reduction of the reactivity to a double integral is possible. Here we have in general two bi-Maxwellian species interacting with each other, for which there does not seem to be a reduction technique available in the literature. Two additional complications arise in the evaluation of the reactivity integral because the distribution functions are drifting and truncated.

In the following we shall confine our calculation to like species fusion interactions, e.g., the D-D reaction rate, be-

cause the common drift speed simplifies our mathematical approach. It is convenient to make two velocity space transformations involving perpendicular and parallel velocity components. The relative velocity components are:

$$\vec{v}_\perp = \vec{v}_{2\perp} - \vec{v}_{1\perp}, \tag{57}$$

$$\vec{v}_\parallel = (v_{2\parallel} - v_{1\parallel})\hat{e}_z, \tag{58}$$

with $\max|\vec{v}_\perp + \vec{v}_\parallel| = \max|\vec{v}| = 2v_{\max}$, and the center-of-mass velocity components are,

$$\vec{v}_{c\perp} = \frac{1}{2}(\vec{v}_{2\perp} + \vec{v}_{1\perp}), \tag{59}$$

$$\vec{v}_{c\parallel} = \frac{1}{2}(v_{2\parallel} + v_{1\parallel})\hat{e}_z, \tag{60}$$

with $\max|\vec{v}_{c\perp} + \vec{v}_{c\parallel}| = \max|\vec{v}_c| = v_{\max}$. Since the Jacobian of the transformation is unity then $d^3\vec{v}_1 d^3\vec{v}_2 = d\chi_c v_{c\perp} dv_{c\perp} dv_{c\parallel} 2\pi v_\perp dv_\perp dv_\parallel$, where χ_c is the angle between $\vec{v}_{c\perp}$ and the radial coordinate.

For the cylindrical expansion $f_1 f_2$ becomes

$$f_1 f_2 = \left(\frac{m_D}{2\pi}\right)^3 \frac{1}{T_\parallel T_\perp^2} \exp\left[\frac{m_s(u_r v_{c\perp}\cos\chi_c - u_r^2)}{2T_\perp}\right] \times \exp\left[-\frac{m_s v_{c\perp}^2 + m_r v_\perp^2}{2T_\perp} - \frac{m_s v_{c\parallel}^2 + m_r v_\parallel^2}{2T_\parallel}\right], \tag{61}$$

where $m_s = 2m_D$, and reduced mass $m_r = m_D/2$. After first performing the integration in the angular variable ($0 < \chi_c < 2\pi$), and then in the variable $v_{c\parallel}$, where $|v_{c\parallel}| < (v_{\max}^2 - v_{c\perp}^2)^{1/2}$, Eq. (55) now reads

$$\langle\sigma v\rangle^{\rm cyn} = \left(\frac{m_D}{2\pi}\right)^3 \frac{C^{\rm cyn}(\nu,\overline{u};\kappa)}{T_\parallel T_\perp^2} \int_{v_\perp} 2\pi v_\perp dv_\perp \times \int_{v_\parallel} dv_\parallel |\vec{v}|\sigma(|\vec{v}|)\exp\left[-\frac{m_r v_\perp^2}{2T_\perp} - \frac{m_r v_\parallel^2}{2T_\parallel}\right]. \tag{62}$$

Here, the $C^{\rm cyn}$ function is an abbreviation for the integral over the variable $v_{c\perp}$ ($0 < v_{c\perp} < v_{\max}$)

$$C^{\rm cyn} = \frac{4\kappa^2}{\nu} e^{-2\vec{u}^2/\nu} \int_0^1 x e^{-2\kappa^2 x^2/\nu} I_0[4\overline{u}\kappa x/\nu] \times \mathrm{erf}[2^{1/2}\kappa(1-x^2)^{1/2}]dx, \tag{63}$$

where I_0 is a modified Bessel function of the order zero, erf is the error function, and we have introduced some important nondimensional parameters,

$$\kappa = v_{\max}/v_{ti} = (E_{\max}/T_*)^{1/2}, \quad \nu = T_\perp(t)/T_*, \quad \overline{u} = u_{ir}(r,t)/v_{ti}, \tag{64}$$

where recall that $E_{\max}$ is defined in Eq. (40). Notice that $C^{\rm cyn} \to 1$ in the limit $v_{\max}, \kappa \to \infty$, reflecting the fact that in this limit we could have computed the reactivity by going into the reference frame moving with the local drift velocity u_{ir}. This would greatly simplify the evaluation of the fusion yield since $\langle\sigma v\rangle$ would have only a temporal dependence, through the temperature $T_\perp$. Unfortunately, this transformation is clearly not expedient when $v_{\max}$ is in reality finite: the time and space dependencies in $\langle\sigma v\rangle^{\rm cyn}$ are actually mixed, making the fusion reactivity and yield calculations more complicated.

Returning to Eq. (62), the remaining integrals over the $\parallel$ and $\perp$ relative velocity components can be done easily by transforming to the spherical polar coordinate system, $2\pi v_\perp dv_\perp dv_\parallel \to 2\pi d\mu v^2 dv (0 < v < 2v_{\max})$, such that $v_\parallel = \mu v$, $v_\perp = (1-\mu^2)^{1/2} v$. The fusion cross sections $\sigma(E)$ are usually expressed in terms of the energy variable $E = m_r v^2/2$. After first performing the integration over the angle coordinate μ, we encounter only the single integral

$$\langle\sigma v\rangle^{\rm cyn} = \left(\frac{2T_*}{m_r}\right)^{1/2} \frac{C^{\rm cyn}(\nu,\overline{u};\kappa)}{(\nu-\nu^2)^{1/2}} \int_0^{2\kappa^2} (-i) \times \mathrm{erf}[i\eta^{1/2}(v^{-1}-1)^{1/2}] e^{-\eta/v}\sigma(\eta T_*)\eta^{1/2} d\eta. \tag{65}$$

A similar reduction can be applied to the cluster expansion in 1D slab geometry. Omitting the details we obtain

$$\langle\sigma v\rangle^{\rm slab} = \left(\frac{2T_*}{m_r}\right)^{1/2} \frac{C^{\rm slab}(\nu,\overline{u};\kappa)}{(1-\nu)^{1/2}} \int_0^{2\kappa^2} \mathrm{erf}[\eta^{1/2}(\nu^{-1}-1)^{1/2}] \times e^{-\eta}\sigma(\eta T_*)\eta^{1/2} d\eta, \tag{66}$$

where in this expression $\nu = T_\parallel(t)/T_* < 1$, and

$$C^{\rm slab} = \frac{\mathrm{erf}[(2/\nu)^{1/2}(\kappa-\overline{u})] + \mathrm{erf}[(2/\nu)^{1/2}(\kappa-\overline{u})]}{2} - \frac{\exp[-2\kappa^2 + 2\vec{\overline{u}}^2/(1-\nu)]}{2(1-\nu)^{1/2}} \times \{\mathrm{erf}[2^{1/2}(\nu-\nu^2)^{-1/2}(\kappa-\kappa\nu-\overline{u})] + \mathrm{erf}[2^{1/2}(\nu-\nu^2)^{-1/2}(\kappa-\kappa\nu+\overline{u})]\}, \tag{67}$$

In order to compare our results with the deuterium-cluster experiments we have used the most up-to-date $D(d,n)^3He$ fusion cross-section formula developed by Bosch and Hale [13]. It is convenient to work with nondimensional notation: $\rho = r/R_0$, $\xi = t/(R_0/v_{ti})$. Noting that $\nu = 1/(1+\xi^2)$, and we can write $\langle\sigma v\rangle^{\rm cyn} = C^{\rm cyn}(\nu,\overline{u};\kappa)S(\xi;\kappa)$. The neutron production rate per unit length z along the plasma filament is the result of the volume integration in Eq. (56), with the cylindrical volume element being $d^3\vec{r} = 2\pi(dz)r\,dr$. After much simplification this is

$$\frac{d^2 N_{\rm neutron}}{dt\,dz} = \frac{2\pi R_0^2 n_{i0}^2 S(\nu;\kappa)}{(1+\xi^2)}\Psi, \tag{68}$$

where

$$\Psi = 16\kappa^2 \int_0^\infty \rho e^{-2\rho^2} \left(\int_0^1 x e^{-2\kappa^2 x^2/v} I_0[4\kappa\xi\rho x] \times \mathrm{erf}[2^{1/2}\kappa(1-x^2)^{1/2}]dx \right) d\rho.$$

Since the ρ integration involving the modified Bessel function I_0 can be done analytically [14], we can reduce the double integral to a single integral that evidently has no time dependence, namely

$$\Psi(\kappa) = 4\kappa^2 \int_0^1 x e^{-2\kappa^2 x^2} \mathrm{erf}[2^{1/2}\kappa(1-x^2)^{1/2}]dx. \quad (69)$$

Since the error function is an integral, we may reverse the order of integration in Eq. (69) to reveal its analytical form

$$\Psi(\kappa) = \mathrm{erf}[(2\kappa^2)^{1/2}] - 2(2\kappa^2/\pi)^{1/2} \exp[-2\kappa^2]. \quad (70)$$

The total neutron yield per unit length z along the plasma filament is finally reduced to a time (or normalized temperature v) integral over the time-dependent part S of the fusion reactivity integral

$$\frac{dN_{\mathrm{neutron}}}{dz} = \left(\frac{R_0}{v_{ti}} \right) (\pi R_0^2) \frac{n_{i0}^2}{4} \Psi(\kappa) \times \int_0^1 S(\nu;\kappa)[\nu(1-\nu)]^{-1/2} d\nu. \quad (71)$$

The physical meaning of the Ψ function is now clear. If we fix the laser intensity, i.e., $E_{\max}$ while increasing the cluster size, or temperature, Ψ decreases monotonically from its asymptotic low-temperature limit, $\Psi \to 1$, $\kappa \to \infty$, to its opposite high-temperature limit $\Psi \to 0, \kappa \to 0$. A similar limiting effect happens to the S function; the number density of ions that can have fusion reactions below the cutoff energy $E_{\max}$ starts to decrease for sufficiently high temperatures. Since S, and the S integral in Eq. (71) contain the fusion cross-section integral, the net result is that the neutron yield has an optimum peak with temperature T_*, or cluster size. Indeed this seems to be the case if we compare our result with the data of Ref. [3].

The present calculations are incomplete, inasmuch as they neglect absorption and attenuation of the laser pulse along the propagation direction, hence κ, actually has a z dependence. In the DZ experiments it was determined that the laser pulse does not fully penetrate to the high-density core of the cluster stream produced by the supersaturated gas jet. Owing to the radial density profile of the gas jet, the initial ion density n_{i0} also varies along the length of the plasma filament. A study of laser absorption in a cluster jet is beyond the scope of this paper, however. Therefore we shall regard κ and n_{i0} as length-average quantities along the plasma filament, and estimate the total neutron yield as $N_{\mathrm{neutron}} \approx (2L_0)(dN_{\mathrm{neutron}}/dz)_{\mathrm{avg}}$.

The initial average ion density is equal to the cluster atom density that was found to be in the range $n_{i0} \sim 2-4 \times 10^{19}\,\mathrm{cm}^{-3}$. Based on the observed plasma filament size, and the estimation of the ionization radius in Sec. II, we estimate that the laser intensity in the cluster plume was in the range $I = 4-8 \times 10^{16}\,\mathrm{W/cm}^2$ (the maximum laser intensity in the vacuum focus was $\geqslant 10^{17}\,\mathrm{W/cm}^2$). In presenting our results we will vary the laser intensity with fixed quantities: $n_{i0} \approx 3 \times 10^{19}\,\mathrm{cm}^{-3}$, $R_0 = 85.5\,\mu\mathrm{m}$, and $2L_0 = 0.2\,\mathrm{cm}$. Figure 1 displays the experimental neutron yield versus the average cluster diameter. The yield ramps up steeply with cluster size and reaches a peak value followed by a roll over. The peak value of the neutron yield occurs at $2r_{\mathrm{avg}} \approx 50$ to 60 Å, and by $2r_{\mathrm{avg}} = 100$ Å the yield has fallen to about one-third of its peak value. Although the scatter in the data is considerable, it appears that our model seems to be in reasonable agreement when we choose $I = 5 \times 10^{16}\,\mathrm{W/cm}^2$. What is clear from the data is that there is a much larger scatter in the neutron signal for the large 100-Å diameter clusters than is present for cluster diameters <40 Å. We believe this is due to that the uncertainty and variation in the light intensity used in the experiments. As shown in Fig. 2 the calculated neutron signal expected from the larger clusters increases much more rapidly with laser intensity than it does for the smaller clusters. However a point of diminishing returns is reached where further increases in the laser intensity do not pay off.

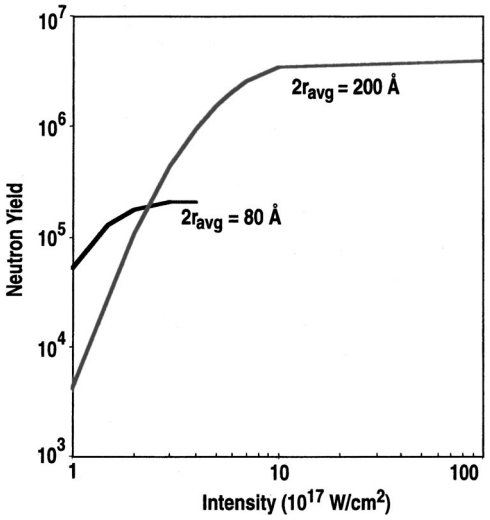

FIG. 2. Calculated neutron yield versus laser intensity for two average cluster sizes $2r_{\mathrm{avg}}$. Plasma filament parameters used are the same as in Fig. 1.

As we might expect, for a given laser intensity the maximum neutron yield is associated with a definite average cluster size, requiring larger sizes for higher laser intensities. Hence, in matters of practical application where it is desirable to maximize the neutron yield, for example, the proper match between cluster size and laser intensity must be taken into account.

VI. CONCLUSION

The major thrust of the present work has been to develop analytical distribution functions for the Coulomb-exploded ions, and from these to analytically determine the D-D fusion neutron reactivity. It provides a framework in which one can

predict the scaling of the present DZ experimental results to larger-sized deuterium clusters and to larger laser energies and intensities. We have calculated the distribution of exploded ions for a given distribution of cluster sizes and found that the temperature T_* of the distribution depends on the average cluster size squared, while the maximum the ion tail energy $E_{\max}$ depends on the laser intensity. As described above, we find that with a reasonable choice for the cluster size distribution produced from the supersaturated gas jet, the resulting ion distributions appear to be Maxwellian-like in form, allowing an analytically tractable solution of the neutron reactivity. Our analysis suggests that a saturation and rollover of the neutron production is expected to occur with increasing average cluster size at a fixed laser intensity, as only clusters up to radius $r_{\max}$ producing ions with maximum energy $E_{\max}$, undergo a full Coulomb explosion. A similar rollover effect is observed in the DZ experiments; the average cluster size at the peak of the neutron yield is in reasonable agreement with this model.

Zweiback *et al.* [3] explained the neutron rollover as being primarily due to enhanced laser absorption in larger-sized clusters. They note that as the cluster size was increased, the plasma filament from the laser-ionized clusters was observed to penetrate somewhat less far into the plume of the gas jet. In the peripheral regions of the gas jet, the average atom density is expected to be lower, and thus the D-D fusion neutron yield $\sim n_{i0}^2$ may be reduced. However, by performing the integrals in Eq. (40), we find that the kinetic-energy density of the Coulomb-exploded ions is $\sim n_{i0} T_* H(\kappa)$, where $H(\kappa)$ is a steeply rising function of the parameter $\kappa=(E_{\max}/T_*)^{1/2}$ for $\kappa<2$. Hence, in the rollover region ($\kappa<1$) the laser energy absorbed by the Coulomb-explosion mechanism actually decreases for larger-sized clusters. Hence collisional absorption must be causing increased laser-light absorption when the cluster size increases.

We should point out some important caveats in our model. First, within our simplified model of the laser-cluster interaction in Sec. II, we have assumed that clusters of radius $r_c \leqslant r_{\max}$ are fully stripped of their electrons. This drives the Coulomb explosion resulting in hot-tail ions up to energy of $E_{\max}$ responsible for the bulk of the neutron-producing fusion events. For clusters of radius $r_c > r_{\max}$ we have assumed that the ionized clusters remain fully neutralized by the oscillating electron cloud, and therefore do not undergo Coulomb explosions. One may allow for collisional heating by inverse bremsstrahlung, during and after which the resulting hydrodynamic pressure drives the expansion of the larger clusters leading to ions of energy $\sim kT_e$. Ambipolar expansion of large rare-gas clusters have been calculated previously (e.g., see Ditmire *et al.* [1]), but for deuterium clusters the collisional heating is much less and one expects deuteron energies of at most only $\sim$200 eV, not sufficient to drive D-D fusion reactions. Consequently, we have so far neglected the production of hot fusion-producing tail ions and fusion neutrons for clusters having initial radius $r_c > r_{\max}$. The motion of the electrons under the action of the strong laser electric field and the strong-Coulomb forces, is considerably more complicated especially when these forces are comparable as they are for $r_c \sim r_{\max}$. We must also consider the partial liberation of some of the electrons from a cluster with radius $r_c > r_{\max}$, and the resulting partial Coulomb explosion. In other words the boundary in terms of cluster radius between the fully exploded clusters and the unexploded clusters is actually fuzzy. One could anticipate that the critical-cluster radius is not so well defined, since the restoring force derived in Sec. II explicitly assumes that the electron-charge distribution remains rigid, uniform, and spherical. As the displacement between the electron and ion clouds becomes appreciable ($\xi \to 1/2$), the electron cloud will distort in shape, thereby lowering the Coulomb-restoring force. In addition, to the extent that the electrons are collisionally heated during the laser pulse, the electron cloud will develop a nonuniform density distribution characterized by the electron temperature and local density. We expect that the width of the boundary in terms of the energy will be of order kT_e. Hence the maximum ion energy would be $\sim E_{\max} + kT_e \approx E_{\max}$, as T_e is estimated to be of order $\sim$100–300 eV.

It has been shown that even with quite modest laser pulses of 0.1 J per pulse, a significant number of fusion neutrons $\sim 10^4$ can be generated by laser-induced Coulomb explosions in solid-deuterium clusters, in agreement with current experiments [3]. Zweiback *et al.* [3] point out that the burst of neutrons from laser-driven Coulomb explosions in cluster media could become a valuable research tool for use in the field of neutron-induced material damage studies. Ultrashort-neutron pump-probe experiments permit time-resolved studies of neutron damage. Such a neutron source would provide valuable information on neutron material damage to fusion-reactor components. These neutron sources become attractive if the neuron flux at a distance of about 1 mm from the source exceeds $10^9\ \mathrm{cm}^{-2}\,\mathrm{s}^{-1}$. To achieve this, we might consider using a 1-J laser with the same pulse width and spot size as used in the DZ experiments. This would lead to a tenfold increase in the laser intensity in the cluster stream, $\sim 5\times 10^{17}\ \mathrm{W/cm}^{-2}$. To optimize the neutron yield at this intensity, this model indicates that the average cluster diameter would have to be fairly large, 176 Å. The combination of this cluster size and laser intensity would dramatically increase the neutron yield to 1.62×10^6 neutrons per pulse. For a repetition rate of 10 Hz, the neutron flux at a distance of about 1 mm from the source would become $4\times 10^9\ \mathrm{cm}^{-2}\,\mathrm{s}^{-1}$, which is more than adequate. In a deuterium-tritium cluster medium the 14.1-MeV fusion neutrons generated could produce the same flux at a distance of 1.4 cm from the source, enabling damage studies in larger samples.

ACKNOWLEDGMENTS

We would like to mention that the ion energy distribution function for a single cluster, Eq. (30), was also derived independently by L. J. Perkins using a different approach. We appreciate helpful discussions with J. Zweiback and T. Ditmire.

[1] T. Ditmire, T. Donnelly, A. M. Rubenchik, R. W. Falcone, and M. D. Perry, Phys. Rev. A **53**, 3379 (1996); J. Zweiback, T. Ditmire, and M. D. Perry, *ibid.* **59**, R3166 (1999).
[2] T. Ditmire, J. Zweiback, V. P. Yanovsky, T. E. Cowan, G. Hays, and K. B. Wharton, Nature (London) **398**, 489 (1999).
[3] J. Zweiback, R. A. Smith, T. E. Cowan, G. Hays, K. B. Wharton, V. P. Yanovsky, and T. Ditmire, Phys. Rev. Lett. **84**, 2634 (2000); J. Zweiback, T. E. Cowan, R. A. Smith, J. H. Hartley, R. Howell, C. A. Steinke, G. Hays, K. B. Wharton, J. K. Crane, and T. Ditmire, *ibid.* **85**, 3640 (2000).
[4] L. J. Perkins *et al.*, Nucl. Fusion **40**, 1 (2000).
[5] P. Mulser, in *Laser Plasma Interactions 5: Inertial Confinement Fusion*, edited by M. B. Hooper (Institute of Physics, Philadephia, 1995), p. 231.
[6] L. V. Keldysh, Zh. Eksp. Teor. Fiz. **47**, 1945 (1964) [Sov. Phys. JETP **20**, 1307 (1965)].
[7] A. M. Perelomov, V. S. Popov, and M. V. Terent'ev, Zh. Eksp. Teor. Fiz. **50**, 1393 1966 [Sov. Phys. JETP **23**, 924 (1966)].
[8] O. D. Jefimenko, *Electricity and Magnetism* (Meredith, New York, 1966), p. 211.
[9] T. G. Kyle, *Atmospheric Transmission* (Pergamon, New York, 1991), p. 64.
[10] R. Narasimha, J. Fluid Mech. **12**, 294 (1962).
[11] I. Nebenzahl, Phys. Fluids **15**, 331 (1972).
[12] W. G. F. Core, Report No. JET-IR **87** 1987 (unpublished).
[13] H.-S. Bosch and G. M. Hale, Nucl. Fusion **32**, 611 (1992).
[14] I. S. Gradshteyn and I. M. Ryzhik *Table of Integrals Series and Products* (Academic Press, New York, 1965).